

PMT Gain Calibration In MicroBooNE

MICROBOONE-NOTE-1064-TECH
MicroBooNE Collaboration

August 6, 2019

1 Introduction

1.1 Uses of light in LArTPC experiments

Liquid argon (LAr) is an ideal scintillating detector medium: it is very bright, releasing $O(10,000)$ photons per MeV of deposited energy, and is also transparent to its own scintillation.

Light data in liquid argon time projection chamber (LArTPC) experiments in general and MicroBooNE in particular has many important uses. In MicroBooNE, light collected over all photosensors is used as a first and second level trigger. At the data acquisition stage ~ 5 PE is required for triggering. An additional software trigger of ≈ 20 PE helps reject a large portion of cosmic ray background in events with no neutrino interaction occurring during the beam spill. Scintillation can also be used for the determination of absolute drift coordinate of non-beam related events. Additionally, matching reconstructed light to reconstructed TPC charge is a powerful tool for cosmic ray rejection. Finally due to the specific properties of LAr scintillation, light information can be used for particle identification. For many of these tasks good modeling of the light response of the detector is crucial. Applying data-driven corrections to optical detector data and simulation (prediction) allows to obtain a well calibrated energy scale from the PMTs. This reduces discrepancies between data and simulation, and calibrates out non-uniformities of data over the full data taking period. Thus it is expected to factor in improving systematic uncertainties on MicroBooNE's flagship analyses - the low energy excess (LEE) (see e.g. [2]) search and LAr- ν cross-section measurements.

1.2 Mechanisms of LAr scintillation

When a charged particle propagates through the TPC volume, it interacts with the LAr medium and either excites or ionizes Ar atoms, which produces scintillation light. There are two main mechanisms of scintillation in LAr: through self-trapping of an excited Ar atom, and through ionization and following re-combination of a thermalized ionization electron. In both cases an excited state (excimer) is formed, which has an Ar_2^+ core and a bound electron. This then de-excites to the dissociative ground state by emitting a UV photon. Excimers exist as a singlet and a triplet state, namely the two lowest-energy states $^1\Sigma_u^+$ and $^3\Sigma_u^+$. The two states have different de-excitation times, resulting in light spectra with different characteristic time constants. The singlet state decays with $\tau \simeq 6$ ns, while for the triplet state $\tau \simeq 1500$ ns. The fraction of prompt (fast) to late (slow) light is dE/dx dependent; for a MIP it is roughly 1 : 3. This dE/dx dependence can be exploited for PID using light. The emitted photons have a wavelength of 128 nm, which is below the energy of the first excited state, thus LAr is largely transparent to its scintillation.

1.3 The light collection system of MicroBooNE

The light collection system of MicroBooNE consists of a primary and a secondary sub-systems. The primary system is made up of 32 optical units, each consisting of a 8 in diameter Hamamatsu R5912-02mod cryogenic PMT behind a TPB-coated acrylic plate and inside a mu-metal shield. The secondary system consists of 4 paddle PMTs. The role of the TPB is to wavelength shift the Ar scintillation to visible light, peaking at 425 nm, well within the sensitive region of the PMTs (Figure 2). The optical sensors are situated in the y-z plane in detector coordinates, mounted on a frame behind the TPC wire readout planes, as can be seen in Figure 1. The cryogenic PMTs are operated at about 1300 V which results in electronic gain of $\approx 10^7$. PMT gain is re-calibrated by minor adjustments to the HV every time the PMT system is turned off (generally a couple times per year), as well as in cases when monitoring shows gains to have shifted out of the (15 – 30) ADC/PE range. For each triggered event, 23.4 μ s of unbiased waveform is recorded. Analog PMT signals pass

through splitter boards, which separate output signal from HV, and are split into a high gain and a low gain channel. The high gain channel carries 18% of the signal amplitude, while the low gain channel carries $\approx 1.8\%$. Having both low and high gain channels allows for waveform substitution in case the high gain waveform is saturated due to a very large light pulse (e.g. after a cosmic muon). Both channels are pre-amplified and shaped before being digitized at 64 MHz. After the shaper signals have a rise time of 60 ns.

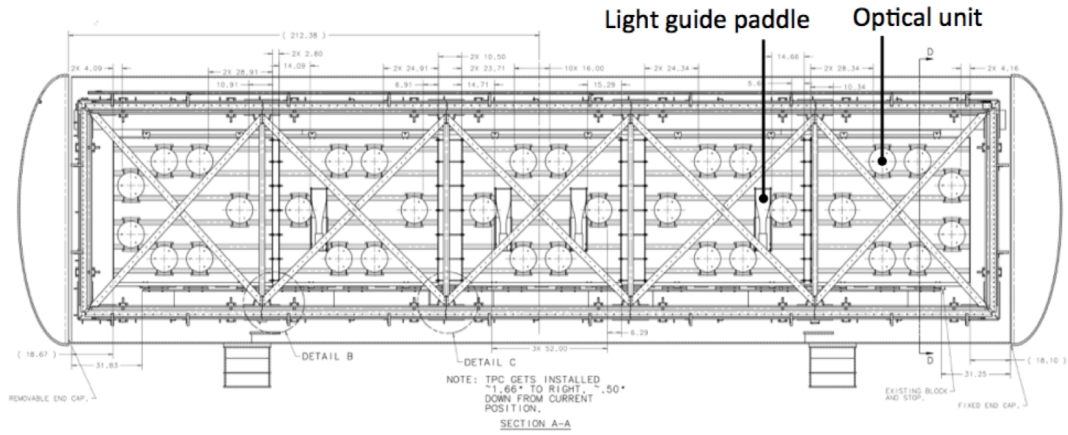


Figure 1: Placement of the light collection system on the frame behind the TPC wire planes. Figure from [1].

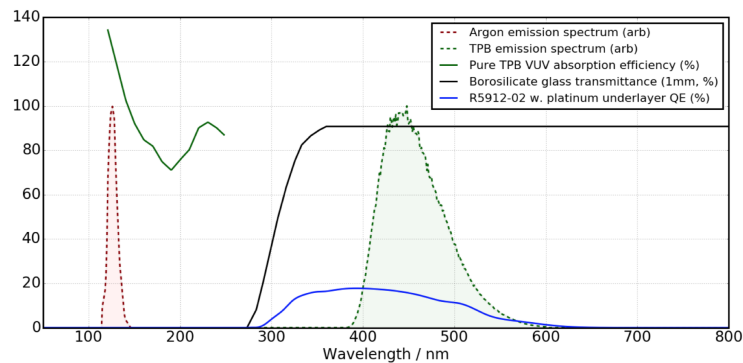


Figure 2: LAr scintillation spectrum, TPB emission spectrum and PMT quantum efficiency as a function of wavelength. Figure from [1].

1.4 Optical reconstruction

Pulse-finding algorithms are applied to every digitized waveform. Light pulses that are isolated in time are reconstructed as optical hits. Hits over all photosensors that are close in time are clustered into optical flashes - objects that represent the light of a single particle interaction in the detector. Flashes can be matched to TPC activity to reject cosmic background. A powerful way to achieve this consists of constructing a hypothesis light spectrum relying on TPC charge information of a reconstructed track or shower and comparing it to reconstructed optical flashes. The hypothesis is based on the theoretical expectation of how much light will be produced by a certain energy deposit, and how this will be distributed among the photodetectors depending on detector geometry. By discarding TPC tracks or showers whose light does not match the optical flash in time with the beam spill, one can reject non-beam related activity.

2 PMT gain measurement using SPE pulses

The integral of a PMT waveform (recorded charge) is proportional to the incident photon flux entering the photosensor. More specifically, the incident light \times photosensor quantum efficiency \times photosensor gain = recorded charge. Gain is often expressed in units of charge recorded per photo electron (PE) produced at the PMT photocathode, or in ADC (units of amplitude) per PE. If one can measure the charge or amplitude of a single photoelectron (SPE) pulse recorded by an optical channel, one can estimate the gain for that specific channel.

2.1 Dataset

Many experiments which employ PMTs use laser or LED light sources to calibrate PMT gain. MicroBooNE is equipped with a flasher LED system [3]. In addition to the LED calibration system, intrinsic sources of SPEs can provide an alternative source of light for calibrations. In MicroBooNE, a SPE noise rate of ≈ 200 kHz has been observed, leading to $O(5)$ SPE pulses per $23.4\mu\text{s}$ of unbiased waveform, as illustrated in Figure 3. Such pulses, while of unknown origin, provide a unique opportunity to measure PMT gains. Using this data has several advantages to the LED flasher system. The pulses are distributed uniformly in the detector volume and over time. Data is recorded as part of MicroBooNE regular physics data taking, and does not require dedicated calibration runs which would disrupt beam data-taking. Hence we have ample statistics spreading over the full data-taking period of the experiment. The dataset we are using for PMT gain calibration is part of the so-called unbiased external data stream, which records signals in anti-coincidence with the neutrino beam without minimum observed light requirement. The unbiased triggering an important condition for gathering low-light pulses.

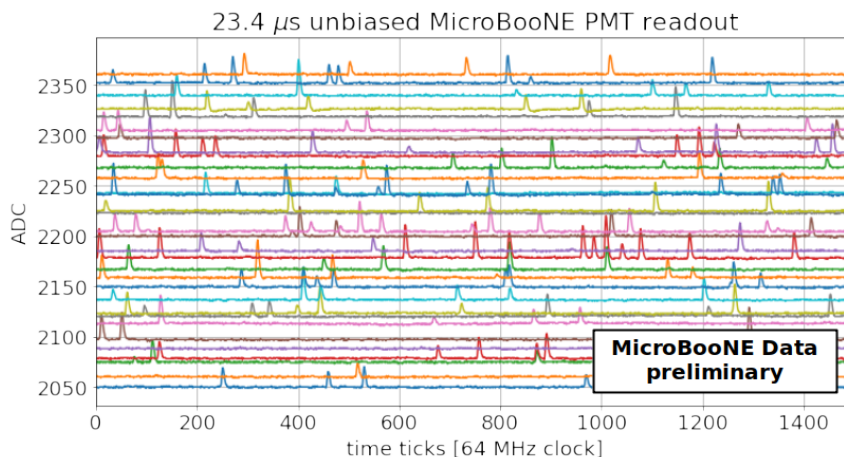


Figure 3: Example of SPE noise in $23.4\mu\text{s}$ unbiased optical readout.

2.2 Pulse finding and signal selection

In order to extract SPE pulses we employ a version of the constant fraction discriminator (CFD) algorithm to the digitized and baseline-subtracted waveforms. This algorithm is chosen because it is well suited for selecting pulses with identical shape but varying amplitude, since it finds pulses based on a constant-fraction w.r.t. maximum threshold. The triggering threshold is set at 10 ADC, which corresponds to ≈ 0.5 PE and is roughly 20 times the RMS of the baseline. This threshold roughly corresponds to the end of the 0 PE peak (pedestal) and is generally far enough from the 1 PE peak (corresponding to mean SPE amplitude), thus it does not compromise our fitting procedure.

In order to exclude baseline fluctuation effects or pulse overlaps, we require that the selected pulses are isolated in time and that averaged baseline is the same before and after the pulse.

To select only well-defined pulses corresponding to order of 1 PE, we further require the following for every pulse:

- amplitude < 50 ADC
- area < 500 ADC \times (time ticks)
- baseline RMS before pulse < 2 ADC
- baseline RMS after pulse < 2 ADC
- $0.95 < \text{ratio of baseline before and after pulse} < 1.05$

2.3 Multi-PE fitting

After the selection we are primarily left with single PE pulses, with some contribution of >1 PE events. In order to extract the PMT gain we need to estimate the mean amplitude (in ADC) or pulse area (in ADC \times time ticks) corresponding to 1 PE. Given the selection applied we assume there is no noise contribution to the observed distribution. In the ideal (no noise) case the number n of PE to reach the first dynode of a PMT for a given number of emitted PE N is described by a Poisson distribution:

$$P(n; N) = \frac{N^n e^{-N}}{n!} \quad (1)$$

The dynode chain amplification response (given the amplification of the first dynode is large) is Gaussian:

$$G(x) = \frac{1}{\sqrt{2\pi\sigma^2}} \exp\left[-\frac{(x - \mu_{\text{SPE}})^2}{2\sigma^2}\right] \quad (2)$$

where x is measured amplitude or pulse area, μ_{SPE} is the mean SPE amplitude, and σ is the intrinsic spread (standard deviation) of the SPE amplitude distribution. Note that pulse amplitude and area are linearly correlated for SPE pulses, since the pulse shape is constant.

The observed amplitude and pulse area distributions are each a convolution of these two responses. Assuming our selected pulses include events with n observed PE, the observed spectra can be represented in the following form:

$$S(x) = \sum_n A_n \frac{N^n e^{-N}}{n!} \frac{1}{\sqrt{2\pi n\sigma^2}} e^{-\frac{(x - \mu_{\text{SPE}n})^2}{2n\sigma^2}} \quad (3)$$

where A_n is the relative normalization of the n PE contribution.

We fit the amplitude and pulse area distributions with this analytical form and extract the mean SPE amplitude (area) parameter μ_{SPE} , which is an effective gain calibration factor. In practice we limit the number of observed PE that we fit to two, due to the selection we apply to the pulses. Figure 4 shows examples of fits for one optical channel. With the current HV setting and electronics in MicroBooNE, mean SPE gains are of the order of 20 ADC/PE (130 ADC \times tick/PE) with $\sim 30\%$ intrinsic spread.

The amplitude and area calibration factors are extracted independently, however the results are linearly correlated, as can be seen in Figure 5. This is an important cross-check of the fitting procedure.

3 PMT gain calibration

3.1 Gain measurements over the period Dec 2015 - Jul 2018

PMT gain is affected by temperature, operating voltage and intensity/frequency of incident light. Gain fluctuations over time can affect the overall light yield (amount of light seen per unit of deposited energy) if not corrected for, and thus can impact both stability of light trigger efficiency, and light-based cosmic rejection. Hence it is important to measure gain evolution over time and

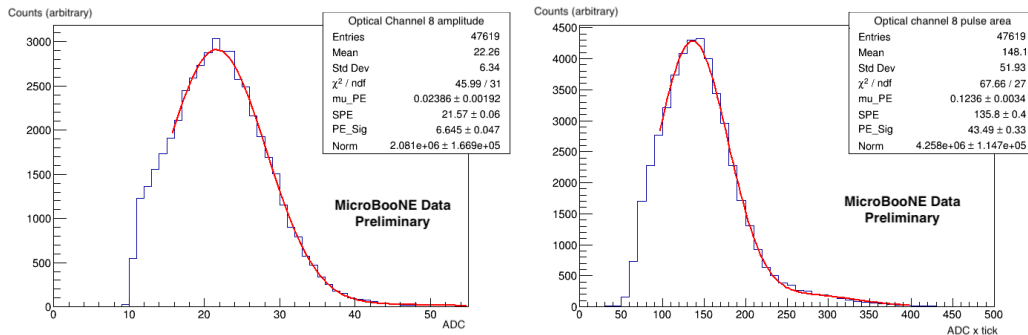


Figure 4: Example of multi-PE fitting on SPE amplitude (left) and area (right).

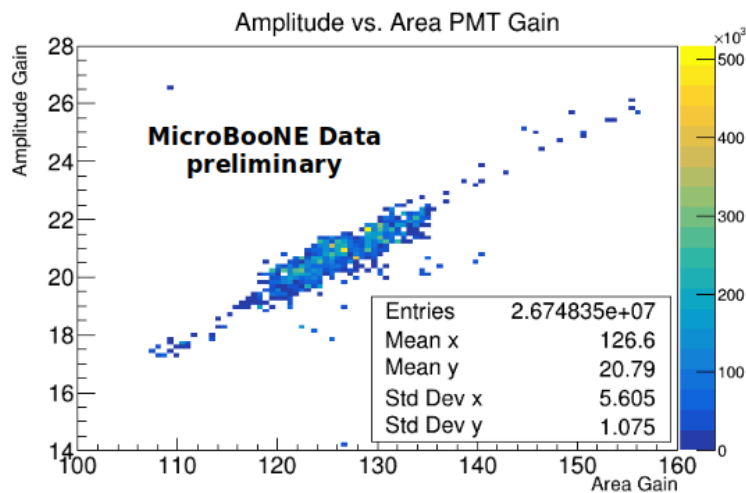


Figure 5: Extracted amplitude gain vs. area gain calibration factors.

account for it in light reconstruction.

PMT gain is measured with the above procedure for data split in one-week-long periods. This time span allows to accumulate enough statistics per period, and is typically short enough to reflect gain fluctuation effects. Figure 6 shows the measured amplitude gain evolution for PMTs numbers 7 through 12, situated in the second downstream PMT rosette on the frame. Measurements for all remaining PMTs can be found in the Appendix, again grouped together by PMT rosettes.

Over the first 6 months since December 2016, gains for optical channels 0 through 7 gradually deviated by up to 30%. The rest of the PMTs also showed a trend of gradual gain change over time, but to a much smaller extent. Taking this into account, MicroBooNE implemented an update in operations procedure at the end of Run 1 of beam data taking in summer 2016. PMT HV was adjusted to constrain all PMTs within a tighter gain range (18-23 ADC/PE) aiming for a mean effective gain of about 20 ADC/PE. Additionally gain stability checks were implemented as part of shifting procedure, where shifters are required to alert relevant experts if an optical channel shows gain outside of the (15-30) ADC/PE range. Finally, a new procedure was implemented after PMT system power-downs, which happen several times a year during detector work. Gains may shift when PMTs are powered down. To account for this, PMT gains are measured after powering back up, and if different from before, HV is adjusted to bring gain back to the values before the power-down.

During Run 2 of beam data taking, most optical channels were stable. A couple of channels, most prominently optical channels 2 and 28, however, had larger gain fluctuations over time. The reason is not fully understood, but it can perhaps be attributed to HV instabilities due to HV channel malfunction or cabling issues. Step-like changes in PMT gain correspond to HV adjustments after PMT system shut-downs.

The period with no data in the plot corresponds to the summer accelerator shutdown after Run 2. During this period optical channel 17 died. PMT HV modules were exchanged with the hope to improve PMT stability. It is clear that this change helped, and all optical channels have been very stable throughout Run3.

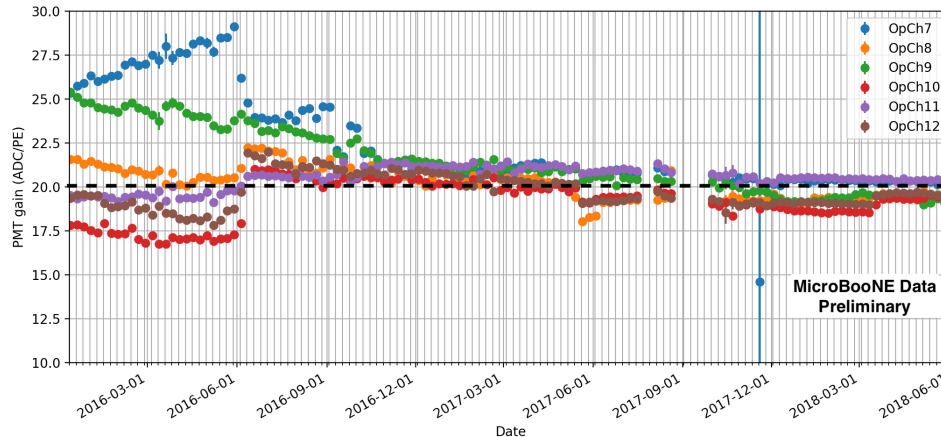


Figure 6: Evolution of PMT gain in MicroBooNE for optical channels 7 through 13 over the period Dec 2015 - July 2018. Each data point corresponds to a one-week period.

3.2 Gain database and application in data analysis

Gain measurements are saved in a conditional database. Each one-week gain measurement corresponds to an interval of validity (IOV). When queried, the database returns values based on which IOV the query timestamp belongs to. This allows to correct optical data with the measured PMT gain that corresponds to the time that data was recorded.

These calibration factors are used in optical flash reconstruction in order to calculate the correct PEs per optical hit at time t :

$$N_Q^{\text{recoPE}}(t) = Q/g^Q(t) \quad (4)$$

$$N_A^{\text{recoPE}}(t) = A/g^A(t) \quad (5)$$

where Q is the integrated optical hit area, A is its amplitude, g are the gain calibration factors extracted by either area or amplitude fitting. Before the implementation of gain corrections number of reconstructed PE was derived using a constant gain of 20 ADC/PE for all optical channels.

4 Performance

We have validated the performance of the gain calibration by comparing observed light (with and without calibration applied) to prediction for TPC anode or cathode crossing cosmic muon tracks. Residuals of observed vs. simulated light over all PMTs are shown Figure 7. Examples over several selected PMTs are shown in Figure 8. Applying the correction minimizes PMT-to-PMT variations in the observed light, thus leading to an overall better agreement between observation and hypothesis. The latter uses a fixed gain of 20 ADC/PE, which causes data to prediction differences if gains are not corrected. It should also be noted that the studies in this section are performed after the overall effect of QE and light mis-modeling across the PMT array are calibrated out.

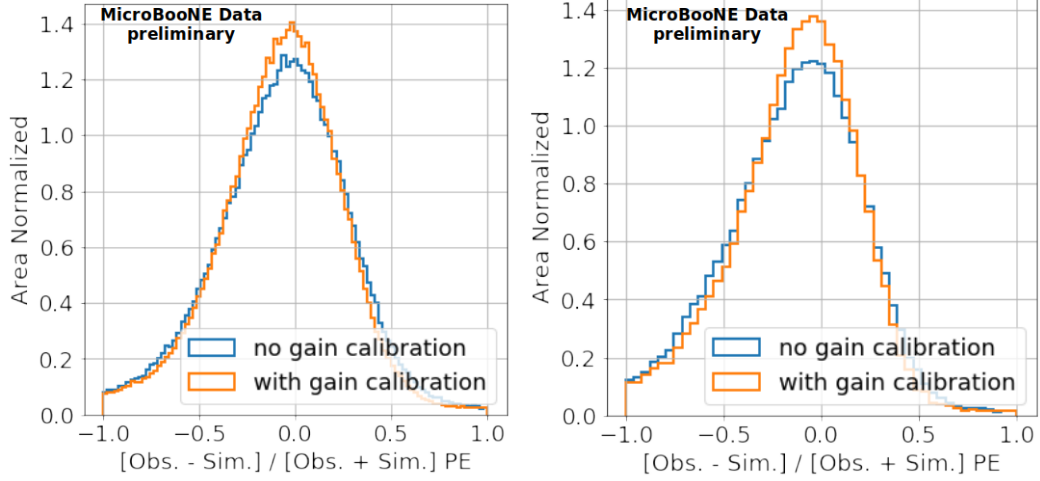


Figure 7: Observed vs. predicted light with and without PMT gain calibration. Left: for full range of reconstructed PE. Right: in the 30-200 reconstructed PE range, to exclude additional reconstruction challenges which occur at low and high PE. Gain correction visibly narrows the distribution.

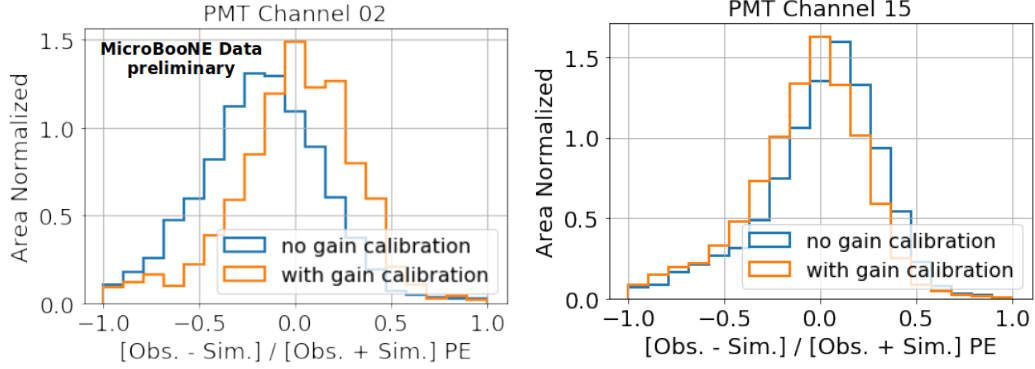


Figure 8: Observed vs. predicted light with and without PMT gain calibration for PMT 2 (left) and PMT 15 (right). Gain correction shifts the distribution, effectively minimizing PMT-to-PMT differences.

5 Summary and conclusions

We have devised a PMT gain calibration procedure which takes advantage of intrinsic single- and few- PE light recorded in MicroBooNE’s optical data. We perform a multi-PE fit to the amplitude and pulse area of those low-intensity light pulses to extract PMT gain calibration factors for each of the 32 PMTs. Gain evolution has been measured over a period of two and a half years from mid-December 2015 to June 2018. After observing gain changes of $O(30\%)$ over the first 6 months of data taking, MicroBooNE implemented changes in operations procedures, which required stricter monitoring and HV adjustments in case of significant gain variations. PMT HV modules were exchanged in early autumn of 2017, which further improved PMT stability to $< \text{few } \%$ variation throughout Run 3 of data taking.

Applying gain corrections in the optical reconstruction visibly improves the stability of the reconstructed light and thus the data to simulation agreement. This is an important first step towards fully characterizing the light response of the MicroBooNE detector.

References

- [1] R. Acciarri et al. (MicroBooNE Collaboration)
Design and Construction of the MicroBooNE Detector
JINST 12 no.02, P02017 (2017)
- [2] A. A. Aguilar-Arevalo et al. (MiniBooNE Collaboration)
Significant Excess of Electronlike Events in the MiniBooNE Short-Baseline Neutrino Experiment
Phys. Rev. Lett. 121, 221801 (2018)
- [3] J. Conrad, B.J.P. Jones, Z. Moss, T. Strauss, M. Toups
The Photomultiplier Tube Calibration System of the MicroBooNE Experiment
JINST 10, T06001 (2015)

Appendices

A PMT gain measurements for PMTs 0-6, 13-31

In this section we show measured PMT gains for the remaining PMTs not shown in the main text.

